

HIGH ENERGY COOLING

V. A. Lebedev[†], Fermilab, Batavia, Illinois, USA

Abstract

The paper reviews methods of particle cooling and their application to future high energy hadron colliders. There are two major types of cooling: the electron cooling and stochastic cooling. The latter can be additionally subdivided on the microwave stochastic cooling (SC), the optical stochastic cooling (OSC) and the coherent electron cooling (CEC). OSC and CEC are essentially extensions of microwave SC, operating in 1-10 GHz frequency range, to the optical frequencies corresponding to 30-300 THz range. The OSC uses undulators as a pickup and a kicker, and an optical amplifier for signal amplification, while the CEC uses an electron beam for all these functions.

INTRODUCTION

In this paper we consider methods of particle cooling applicable for high energy heavy particles (protons or ions) in the high energy colliders. Further in all equations we assume protons – the most challenging case. To transit to ions, one needs to replace in the below equations, as appropriate, the proton classical radius r_p by $Z^2 r_p / A$, where Z and A are the charge and mass numbers of ion. Presently, there are two major methods of cooling: the electron cooling [1] and the stochastic cooling [2]. Up to recently, the stochastic cooling has been only operating at the microwave frequencies. A transition to much higher optical frequencies should enable much faster cooling of dense colliding bunches. The stochastic cooling at extremely high (optical) frequencies can be additionally subdivided into the optical stochastic cooling (OSC) [3] and the coherent electron cooling (CEC) [4]. OSC and CEC are essentially extensions of microwave stochastic cooling operating in the 1-10 GHz frequency range to the optical frequencies corresponding to the 30-300 THz range. At these frequencies one cannot use usual electro-magnetic pickups and kickers. Instead, the OSC uses undulators for both the pickup and the kicker, and an optical amplifier for signal amplification; while the CEC uses an electron beam for all these functions.

The electron and stochastic cooling are based on completely different principles. The electron cooling is dissipative in its principle of operation and therefore the Liouville theorem is not applicable. That enables direct reduction of the beam phase space. The stochastic cooling is a Hamiltonian process which formally does not violate the Liouville theorem and cooling happens due to the phase space reconfiguration so that phase space volumes containing particles are moved to the beam center while the rest mostly moves out. That makes stochastic cooling rates strongly dependent on the beam particle density. As one will see below each method has its own domain where it achieves a superior efficiency. The electron cooling is preferred at a small energy, and its efficiency weakly depends on the particle density in the cooled beam; while the stochastic cooling is

preferred at a high energy, but its efficiency reduces fast with increase of particle density.

HIGH ENERGY ELECTRON COOLING

The highest energy electron cooling achieved to the present time is 4.3 MeV [5, 6]. It was used in Tevatron Run II for cooling 8 GeV antiprotons. The electron beam was accelerated in an electrostatic accelerator. The maximum beam current was 500 mA. The typical beam current used for antiproton storage was about 100 – 200 mA. That supported beam cooling time of about 20 min.

A transition to high energy colliders like Electron-Ion Collider [7] requires the electron beam energy above tens of MeV. That is impossible to achieve with electrostatic acceleration. Consequently, two radically different approaches to the beam acceleration were suggested. The first one suggests using the energy recovery superconducting linac [8], while the second approach uses an induction linac with electron beam injection into a ring where the electron beam circulates for many thousands turns [9]. That allows one to reduce the electron beam power to acceptable level. Reference [10] considers another modification of ring-based cooler where the cooling electron beam is cooled by its synchrotron radiation. That drops the frequency of reinjections and results in an additional reduction of linac power.

Before we consider these schemes, we need to write down equations for the cooling rates of relativistic beams. The corresponding derivations were carried out in Ref. [8]. They assume the Gaussian distributions for both the electron and proton beams and non-magnetized cooling. In all practical cases the longitudinal velocity spread is much smaller than the transverse one. Then the corresponding longitudinal and transverse emittance cooling rates for $\Theta_{\parallel} / (\gamma \Theta_{\perp}) \leq 2$ can be approximated, with accuracy better than few percent, as following:

$$\lambda_{\parallel} \equiv \frac{1}{\theta_{\parallel p}^2} \frac{d}{dt} \theta_{\parallel p}^2 \approx \frac{4\sqrt{2}\pi n_e r_e r_p L_c}{\gamma^4 \beta^4 (\Theta_{\perp} + 1.083 \Theta_{\parallel} / \gamma)^{3/2} \sqrt{\Theta_{\perp} \Theta_{\parallel}}} L_{cs} f_0, \quad (1)$$

$$\lambda_{\perp} \equiv \frac{1}{\theta_{\perp p}^2} \frac{d}{dt} \theta_{\perp p}^2 \approx \frac{\pi\sqrt{2}\pi n_e r_e r_p L_c}{\gamma^5 \beta^4 \Theta_{\perp}^2 (\Theta_{\perp} + \sqrt{2} \Theta_{\parallel} / \gamma)} L_{cs} f_0.$$

Here $\Theta_{\parallel} = \sqrt{\theta_{\parallel e}^2 + \theta_{\parallel p}^2}$, $\Theta_{\perp} = \sqrt{\theta_{\perp e}^2 + \theta_{\perp p}^2}$ are the effective longitudinal and transverse rms momentum spreads, $\theta_{\parallel p,e} \equiv \sqrt{\Delta p_{p,e}^2} / p_{p,e}$ and $\theta_{\perp p,e} \equiv \sqrt{\Delta p_{\perp p,e}^2} / p_e$ are the relative longitudinal and transverse rms momentum spreads in the proton/electron beam, γ and β are the relativistic factors, $n_e = \gamma n'_e$ is the electron beam density in the lab frame, r_e is the classical electron radius, L_c is the Coulomb logarithm, L_{cs} is the cooling section length, and f_0 is the revolution frequency for protons. These equations imply that the proton

[†] valebedev@jinr.ru

beam is completely inside electron beam, and that for each beam (electron or proton) the horizontal and vertical rms transverse angles are equal.

To make a simple best-case estimate, we assume that the proton beam is focused to the center of cooling section with equal transverse β -functions; both transverse and longitudinal rms angles in the electron beam are much smaller than in the proton beam; the cooling length is twice larger than the β -functions of proton beam in the cooling section center; and the electron beam radius is 2 times larger than the rms proton beam size in the center. The latter requirement is determined by a necessity to cool high amplitude particles. In relativistic colliders the longitudinal effective momentum spread is small and the second terms in parentheses of Eqs. (1) can be neglected. As result we obtain:

$$\lambda_{||} = \frac{2\sqrt{2}r_e r_p \beta^* L_c}{\sqrt{\pi} \gamma^2 \beta^2 \varepsilon_{pn}^2 \theta_{||p} C} \frac{I_e}{e}, \quad \theta_{||} \ll \gamma \theta_{\perp}.$$

$$\lambda_{\perp} = \sqrt{\frac{\pi}{2}} \frac{r_e r_p \beta^{3/2} L_c}{\gamma^{5/2} \beta^{3/2} \varepsilon_{pn}^{5/2} C} \frac{I_e}{e}, \quad (2)$$

Here e is the electron charge, C is the proton ring circumference, ε_{pn} is the rms normalized proton emittance, I_e is the electron beam current, and we assume uniform density distribution across the electron beam. For eRHIC parameters [11] (proton beam β -functions in cooling section center - 60 m, total cooling length - 120 m, proton beam energy - 275 GeV, rms normalized emittance - 2.7 μm , ring circumference - 3.8 km) and the electron beam of 100 A one obtains the transverse cooling time of ~ 50 min. The longitudinal cooling strongly depends on the momentum spread in the proton beam. For the rms momentum spread of $5 \cdot 10^{-4}$ one obtains the longitudinal cooling time of about 5 min. Accounting the momentum and angular spreads in the electron beam increases the cooling times by at least 2 times.

The IBS represents a major heating mechanism which has to be counteracted by beam cooling. A simple estimate of IBS emittance growth rates for ultrarelativistic beam with $\gamma \gg \nu_x$ directly follows from Eq. (11) of Ref. [12]. In smooth lattice approximation we assume equal betatron tunes $\nu_x \approx \nu_y$, and beta-functions $\beta_x \approx \beta_y \approx R_0 / \nu_x$. That yields $\sigma_x \approx \sigma_y \approx \sqrt{\varepsilon_{pn} \beta_x / \gamma}$, $\theta_{xp} \approx \theta_{yp} \approx \sqrt{\varepsilon_{pn} / (\beta_x \gamma)}$, $D_x \approx R_0 / \nu_x^2$ and the emittance growth rates:

$$\begin{pmatrix} \lambda_x \\ \lambda_y \\ \lambda_p^2 \end{pmatrix} \approx \frac{N_p r_p^2 c L_{cp}}{8 \sqrt{\gamma} \sigma_z \varepsilon_{pn}^2} \begin{pmatrix} \sqrt{R_0 / (\varepsilon_{pn} \nu_x^5)} \\ 0 \\ (\sqrt{\nu_x \varepsilon_{pn} / R_0}) / (\gamma \theta_{||p}^2) \end{pmatrix}. \quad (3)$$

Here $R_0 = C/2\pi$, c is the speed of light, N_p is the number of particles in a bunch, L_{cp} is the Coulomb logarithm, and σ_z is the rms bunch length.

In Eq. (2) we assumed that the velocity spreads of electrons are much smaller than protons. While it maximizes the cooling rates it creates a problem of overcooling, resulting in the beam distribution with peak in the center. That greatly amplifies the beam-beam and space charge effects and worsens the beam lifetime. Note also that even in the absence of beam-beam effects there is no a stationary

solution (resulting the beam loss) of Fokker-Planck equation if at large action the ratio $\lambda(I)/D(I)$ decays faster than $1/I$ (or $1/I^2$). Here I is the transverse motion action, $\lambda(I)$ is the cooling rate, and $D(I)$ is the diffusion. The ratio of considered above IBS diffusion and cooling rate is close to this boundary.

As one can see from Eqs. (2) and (3) for fixed normalized emittances, electron beam current and particle number in a bunch the transverse cooling rate decreases with energy as $1/\gamma^{5/2}$, while the heating rate as $1/\sqrt{\gamma}$. Consequently, the electron beam current must grow at least as γ^2 , and the electron beam reactive power as γ^3 . That limits the electron cooling of proton beams by energy ~ 200 – 300 GeV where ~ 100 A peak current and multi-gigawatt reactive power of electron beam are required. Such power can be achieved only in the case of effective energy recuperation reducing the actual power transferred by beam to accelerator by at least 3-4 orders of magnitude. Two basic scenarios were recently considered: one based on beam acceleration in a superconducting energy recovery linac and another one on the acceleration in an induction linac.

A usage of the energy recovery linac enables to have bunched electron beam with bunches coinciding in time and duration with proton bunches. That reduces the average beam current by about an order of magnitude. Another 2-3 orders still have to be obtained from the energy recovery which does not look realistic if applied directly. An electron beam storage in a storage ring for tens of turns could address this problem [10]. The number of turns is determined by emittance growth driven by coherent synchrotron radiation. Also there has to be addressed a long-standing problem with reliable production of short and intense bunches from photocathode, since required bunch length cannot be obtained from thermal cathode.

To avoid problems with impedances, CSR and photocathode lifetime Ref. [9] suggests to use an induction linac accelerating the beam from a thermal cathode, immersed into a longitudinal magnetic field, and injecting the beam into a storage ring with long straight section where the protons and electrons move together. Careful design of optics for the electron gun, the beam transport and the ring enabled to obtain the angular spread and beam size required for cooling. The ring optics is based on Derbenev's adaptors. That yielded significant reduction of IBS and the betatron tune shifts driven by space charge. The longitudinal magnetic field in the cooling section compensates vortex created by the cathode magnetic field. The field is chosen so that to obtain an integer number of Larmor rotations in the cooling section to minimize electron beam heating by proton bunches. These measures enabled to minimize problems with impedances and beam space charge and obtain the emittance growth time of about 10,000 turns mainly driven by IBS in electron beam.

Another proposal [13] suggests to add strong wigglers to the ring to amplify synchrotron radiation damping so that it could counteract IBS in the electron beam. In this case the length of accumulated bunch is matched to the proton bunch length. That greatly mitigates the mentioned above

problem with CSR. However, there are severe problems with beam stability which needs to be addressed. If successful the time of beam reinjection will be determined by Touschek scattering. That promises a great reduction of beam power.

OPTICAL STOCHASTIC COOLING

All standard microwave stochastic cooling methods are based on a subtraction of two signals: signals of two pickup plates in the Palmer or transverse cooling, and signals of two consecutive turns in the filter cooling. Consequently, the reference particle does not create a signal on the kicker. That not only reduces the power of kicker amplifier but also reduces the diffusion introduced by cooling system, thus resulting faster cooling. However, in transition from the microwave frequencies to the optical frequencies we lose ability to create difference signals similar to the microwave cooling. In this case the transit-time cooling is the only practical choice. In the transit-time cooling the reference particle does not experience a kick because it comes at the right time when the kicker voltage excited by this particle is equal to zero. Particles which experience oscillations relative to the reference particle are coming at different times and therefore experience corrective kicks.

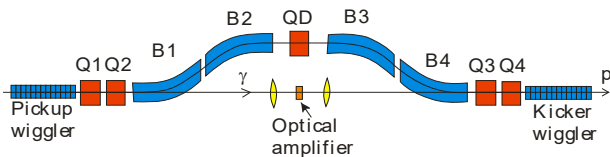


Figure 1: Layout of the OSC system.

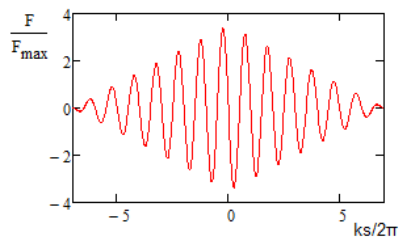


Figure 2: Dependence of cooling force on the longitudinal particle position relative to the reference particle for a 7-pole undulator.

In the optical stochastic cooling (OSC) [3] a particle radiates electromagnetic wave in the first (pickup) undulator (PU). Then, this wave is amplified in an optical amplifier (OA) and focused to the second (kicker) undulator (KU) as shown in Fig. 1. The particle beam is separated from the radiation by a dipole chicane creating space for OA and optical lenses. The chicane introduces a delay equal to a delay of radiation in the optical system, so that a particle would interact with its own radiation amplified by OA. In further consideration we assume that the chicane is in the horizontal plan and there are no x - y coupling terms in the chicane. Figure 2 shows a dependence of longitudinal kick on the longitudinal particle position in KU. Note that for optical frequencies and ultra-relativistic beams the trans-

verse kicks are strongly suppressed. Therefore, to create transverse cooling one needs to couple longitudinal and transverse motions. That is achieved by introduction of non-zero dispersions in PU and KU which introduces a dependence of longitudinal particle position on the betatron motion and thus couples x and s planes.

Balance between cooling of a given particle (proportional to the system gain) and this particle heating by field of other particles (proportional to the gain squared) determines the optimal gain and maximum achievable longitudinal cooling rate per turn (see Appendix in [14]):

$$\lambda_{s_opt} = \frac{3\mu_{01}^2 k_0 \sigma_z}{2\sqrt{\pi} n_w N_p n_\sigma^2} \cdot \quad (4)$$

Here $n_\sigma = (\Delta p / p)_{max} / \sigma_{\parallel p}$ is the ratio of the cooling range in momentum to the rms momentum spread, μ_{01} is the first root of Bessel function $J_0(x)$, k_0 is the wave number for forward radiation, and n_w is the number of poles in the undulator. Eq. (4) implies that the bandwidths of OA and the optical system are wider than the bandwidth determined by the number of undulator periods. For frequency response similar to the presented in Fig. 2 the relative bandwidth is $\Delta f_{FWHM} / f = 0.88 / n_w$. Using this equation one can rewrite Eq. (4) in the following form:

$$\lambda_{s_opt} \approx 35 \frac{\sigma_z \Delta f_{FWHM}}{c N_p n_\sigma^2} \cdot \quad (5)$$

Table 1: Tentative Parameters of OSC

Parameter	Value
Basic wavelength of forward radiation	5.5 μm
Band of optical amplifier, μm	5.4-6.6
Number of undulator periods	20
Peak undulator magnetic field	10 T
Length of undulator period	0.907 m
Undulator parameter	0.46
Angle subtending PU outgoing radiation	1.6 mrad
M_{56} (PU-to-KU transfer matrix element)	3.3 mm
Gain of optical amplifier, dB	50
Emittance cooling times, $\tau_x / \tau_y / \tau_s$, min	30/30/30
Power of optical amplifier	<500 W

Equation (5) is applicable in the general case of bunched beam subjected to the transit-time cooling. It is important to note that in Eqs. (4) and (5) the cooling rate depends on n_σ . This is always the case for the transit-time cooling. For the Electron-Ion collider with $N_p = 6.9 \cdot 10^{10}$, 20-pole undulators, basic wavelength of 5.5 μm and $n_\sigma = 4$ we obtain the emittance cooling time at the optimal gain equal to 15 min. Table 1 presents the major parameters of the OSC system which could support beam cooling in the Electron-Ion-collider at 275 GeV. Calculations were done with theoretical background developed in Ref. [14]. As one can see for the chosen gain of OA the cooling rates are still twice smaller than at the optimal gain, i.e., the noise of nearby particle still has small effect on cooling. The element M_{56} of 6D transfer matrix from PU to KU determines the cooling

ranges and cooling dynamics. It was chosen to support 3D cooling.

Experimental study of OSC was carried out in Fermilab [15]. It showed the performance close to the theory prediction. The layout of Fermilab OSC straight is shown in Fig. 1. Dipoles B1 – B4 are rectangular. Consequently, for zero strength of coupling quad, QD, there is no coupling between longitudinal and transverse planes. Powering of QD results in coupling and transverse cooling. Since in this case the sum of cooling rates is constant, changes in QD may set the required ratio of cooling rates. The vertical cooling rate is introduced by operation in vicinity of coupling resonance. 3D OSC cooling was demonstrated in experiments. Required strength of QD is quite small. From the beam optics point of view, it is the simplest possible scheme and therefore this scheme was chosen for the Fermilab experiment where a passive scheme (no OA) was used to minimize delay in the optical system. However, this simplicity of chicane has a serious drawback. Such design binds M_{56} and the delay in the chicane, Δs , so that $\Delta s = M_{56}/2$. For M_{56} presented in Table 1 it yields the delay of 1.5 mm which may be insufficient for 50 dB amplifier. If this is the case more complicated design is required where additional quads are engaged. It is certainly possible but will make tuning of the line much more sensitive to errors.

COHERENT ELECTRON COOLING

The coherent electron cooling (CEC) [16] was suggested to address the fast decrease of electron cooling force with increase of proton velocity. First attempts to find a practical scheme were aimed at relatively small energy and did not deliver a practical scheme. The breakthrough happened at the end of 2000's with transition to relativistic energies and a suggestion to use FEL (free electron laser) as an amplifier [17]. That addressed the main problem of CEC how to switch on and switch off amplification in controllable fashion. However, after careful examination it was understood that the narrow band of FEL (~0.5%) and a quite short length of the electron bunch (~1/100 of proton bunch length) limit cooling rates to approximately the same level as it was already achieved in the bunched beam microwave stochastic cooling at RHIC [18]. Further investigations of CEC revealed two other schemes which are expected to have much wider bandwidth (up to ~50%). They are the micro-bunched electron cooling [19] and the cooling based on the plasma-cascade instability [20]. All mentioned above cooling schemes operate at the same principle as the SC and therefore can be described within the same theoretical framework. Similar to the OSC the CEC is based on the longitudinal kicks. Consequently, the transverse cooling is achieved by coupling transverse and longitudinal degrees of freedom as described in the OSC section above.

All existing proposals of CEC are based on superconducting energy recovery linacs [21] which can deliver required transverse emittances and momentum spreads, but cannot deliver sufficiently large number of particles in the bunch. To create a desired amplification, one need to have large peak current. As result the electron bunch length is much shorter than the proton bunch length. That, as will be

seen below, reduces the cooling rates in proportion of bunch length ratio.

Following a standard recipe in which one compares the total cooling and heating powers, assuming Gaussian particle distributions in both the electron and proton bunches one estimates the optimal gain and related cooling rate:

$$\lambda_{\max} \approx 2\pi^2 \sqrt{\pi} \frac{\sigma_z W_{\text{eff}}}{c N_p n_\sigma^2} \frac{\sigma_g}{\sqrt{\sigma_g^2 + \sigma_z^2}}. \quad (6)$$

Here $W_{\text{eff}} = \left(\int_0^\infty \text{Re}(G(f)) df \right)^2 / \int_0^\infty |G(f)|^2 df$ is the effective bandwidth of cooling system, $G(f)$ is the dependence of its gain on frequency, and σ_g is the rms gain length which for small gain coincides with rms length of electron beam. In Eq. (6) we neglect the noise present in the electron beam and ignore that the cooling which is present only in the center of proton bunch makes the longitudinal distribution non-Gaussian with sharp peak in the center and long tails. Equations (6) and (5) coincide for $\sigma_g \gg \sigma_z$ if one accounts a difference in the bandwidth definitions.

In further estimates we assume the electron bunch parameters of Ref. [22]: $\sigma_g = 4$ mm, the number of electrons per bunch - $N_e = 6.3 \cdot 10^9$, and the rms beam size - $\sigma_\perp = 0.6$ mm. We do not consider each CEC scheme in detail, but rather list phenomena which are common for all schemes and which represent major limitations on the cooling rates.

A saturation of CEC amplifier represents a severe limitation. Calculations in a single dimensional model exhibit that for parameters of Ref. [22] the rms density fluctuations achieve 18%. The linearity of plasma response will be lost with such large density perturbation. 1D model shows that this is not a problem for cooling, however 3D modelling is required to make sure that this is acceptable.

All calculations neglect noise in the electron beam while measurement showed that it may be the dominant effect. Any sharp perturbation in the electron beam density will result in cooling rate reduction. The gain narrowing associated with electron bunch length also needs to be accounted. It is also amplified by non-uniform density distribution. To be convincing the answers to the listed above problems must be obtained experimentally.

CONCLUSION

The beam cooling of proton bunches in the high energy hadron colliders is one of the most challenging problems in the modern accelerator physics. Although considerable progress has been achieved in the recent years there is a number of problems which need to be addressed before a real cooler can be built.

The electron cooling looks as a possible technology for the proton beam energy below ~250-300 GeV. Presently, only ring-based cooling looks feasible for the proton energies above ~100 GeV. With lowering energy, a cooler based on the energy recovery linac looks as a possibility due to significant reduction of required electron beam current.

The OSC looks as an extremely promising technology for the proton beam energy above ~250-300 GeV.

However, it requires the state-of-the-art undulators with field of ~ 10 T, and an optical amplifier with small signal delay and large gain. The passive OSC was demonstrated in the IOTA ring in Fermilab with 100 MeV electrons. That strongly supports further developments and assures us that the stochastic cooling at the optical frequencies is possible.

The CEC development is still at its initial stage. Although considerable work has been done in recent years its potential and reach needs to be understood better before real implementation can be considered.

REFERENCES

- [1] G. I. Budker, in *Proc. Int. Symp. on Electron and Positron Storage Rings*, Saclay, 1966, *Atomnaya Energiya*; vol. 22, p. 346, 1967,
- [2] Van der Meer, “Stochastic damping of betatron oscillations”, CERN, Geneva, Switzerland, Internal Rep. CERN/ISR PO/72-31.
- [3] M. S. Zolotarev and A. A. Zholents, “Transit-time method of optical stochastic cooling”, *Phys. Rev. E*, vol. 50, no. 4, p. 3087, 1994.
- [4] Y. S. Derbenev, “On possibilities of fast cooling of heavy particle beams”, *AIP Conf. Proc.*, vol. 253, p. 103, 1992. doi:10.1063/1.42152
- [5] *Fermilab Recycler Ring Technical Design Report*, Fermilab, Batavia, IL, USA, Rep. FERMILAB-TM-1991, Nov. 1996,
- [6] S. Nagaitsev *et al.*, “Experimental demonstration of relativistic electron cooling”, *Phys. Rev. Lett.*, vol. 96, p. 044801, 2006. doi:10.1103/PhysRevLett.96.044801
- [7] The Electron-Ion Collider, <https://www.bnl.gov/eic/>
- [8] H. Zhang, S. V. Benson, Y. S. Derbenev, Y. Roblin, and Y. Zhang, “Multi-stage electron cooling scheme for JLEIC”, in *Proc. IPAC'18*, Vancouver, BC, Canada, Apr.-May 2018, pp. 397-399. doi:10.18429/JACoW-IPAC2018-MOPML006
- [9] V. Lebedev *et al.*, “Conceptual design report: A ring-based electron cooling system for the EIC”, *J. Instrum.*, vol. 16, p. T01003, 2021. doi:10.1088/1748-0221/16/01/T01003
- [10] H. Zhao, J. Kewisch, M. Blaskiewicz, and A. Fedotov, “Ring-based electron cooler for high energy beam cooling”, *Phys. Rev. Accel. Beams*, vol. 24, p. 04350, 2021. doi:10.1103/PhysRevAccelBeams.24.043501
- [11] C. Montag *et al.*, “eRHIC design overview”, in *Proc. IPAC'19*, Melbourne, Australia, May 2019, pp. 794-796. doi:10.18429/JACoW-IPAC2019-MOPRB093
- [12] V. Lebedev *et al.*, “Intrabeam scattering and stripping, Touschek effect” in A. Chao, *et al.* “Handbook of accelerator physics and engineering”, World scientific, 2022.
- [13] H. Zhao, J. Kewisch, M. Blaskiewicz, and A. Fedotov “Ring-based electron cooler for high energy beam cooling”, *Phys. Rev. Accel. Beams*, vol. 24, p. 043501, 2021. doi:10.1103/PhysRevAccelBeams.24.043501
- [14] V. Lebedev, J. Jarvis, H. Piekarz, A. Romanov, J. Ruan, and M. Andorf, “The design of Optical Stochastic Cooling for IOTA”, *J. Instrum.*, vol. 16, no. 5. P. T05002, May 2021. doi:10.1088/1748-0221/16/05/T05002
- [15] J. Jarvis *et al.*, “Experimental demonstration of optical stochastic cooling”, *Nature*, vol. 608, pp. 287–292, 2022. doi:10.1038/s41586-022-04969-7
- [16] Y. S. Derbenev, “On possibilities of fast cooling of heavy particle beams”, *AIP Conf. Proc.*, vol. 253, pp. 103-110, 1992. doi:10.1063/1.42152
- [17] V. N. Litvinenko and Y. S. Derbenev, “Coherent electron cooling”, *Phys. Rev. Lett.*, vol. 102, p. 114801, 2009. doi:10.1103/PhysRevLett.102.114801
- [18] J. M. Brennan, M. Blaskiewicz, and F. Severino, “Successful bunched beam Stochastic Cooling in RHIC”, in *Proc. EPAC'06*, Edinburgh, UK, Jun. 2006, pp. 2967-2969, <https://accelconf.web.cern.ch/e06/PAPERS/THPCH078.PDF>
- [19] D. Ratner, “Microbunched electron cooling for high-energy hadron beams”, *Phys. Rev. Lett.*, vol. 111, p. 084802, 2013. doi:10.1103/PhysRevLett.111.084802
- [20] V. Litvinenko *et al.* “Plasma-cascade instability”, *Phys. Rev. Accel. Beams*, vol. 24, p. 014402, 2021. doi:10.1103/PhysRevAccelBeams.24.014402
- [21] A. Bartnik *et al.*, “CBETA: First multipass superconducting linear accelerator with energy recovery”, *Phys. Rev. Lett.*, vol. 125, p. 044803, 2020. doi:10.1103/PhysRevLett.125.044803
- [22] S. Nagaitsev, V. Lebedev, G. Stupakov, E. Wang, and W. Bergan, “Cooling and diffusion rates in coherent electron cooling concepts”, Fermilab, IL, USA, Rep. FERMILAB-CONF-21-054-AD. doi:10.48550/arXiv.physics/2102.10239